Proceedings of the 49th International School and Conference on the Physics of Semiconductors "Jaszowiec 2021"

AlGaN Composition Correction under Variable Ammonia and Pressure Conditions in MOVPE Reactor

K. Moszak[a,b,*], W. Olszewski[a,c], D. Pucicki[a,d], J. Serafińczuk[a,c], K. Startek[a,b] and D. Hommel[a,d]

[a] *Łukasiewicz Research Network -PORT Polish Center for Technology Development, Stabłowicka 147, 54-066 Wrocław, Poland*
[b] *Institute of Low Temperature and Structure Research, Polish Academy of Sciences W. Trzebiatowski Institute, Okólna 2, 50-422 Wrocław, Poland*
[c] *Institute of Experimental Physics, University of Wrocław, Maksa Borna 9, 50-204 Wrocław, Poland*
[d] *Department of Nanometrology, Wrocław University of Science and Technology, Janiszewskiego 11/17, 50-372 Wrocław, Poland*

Doi: 10.12693/APhysPolA.141.105 *e-mail: karolina.moszak@port.lukasiewicz.gov.pl

Growth characteristics of AlGaN layers in different conditions: pressure and ammonia flow were presented. The structures containing the AlN buffer and the AlGaN layer were grown by metalorganic vapor phase epitaxy. The goal was to find the growth conditions for AlGaN with stable 60% of aluminium and determine the aluminium concentration deviation while changing two parameters. Pressure showed bigger influence on aluminium incorporation, layer quality and surface roughness than ammonia.

topics: MOVPE, AlGaN 60%, concentration adjustment, UV LED

1. Introduction

III-nitrides materials are nowadays commonly used in technology due to their wide range of applications in the fields of optoelectronics and electronics e.g. ultraviolet light-emitting diodes (UV-LED) or fast switching transistors [1–7]. Semiconductor structures often consist of ternary compounds due to the changeable bandgap [8]. One of the examples is aluminium gallium nitride (AlGaN) alloy which is a semiconductor with a wide and direct bandgap. Ultraviolet light emitting diode (UV-LED) works on AlGaN-based materials that are mainly prepared by metalorganic vapor phase epitaxy (MOVPE). Commonly UV-LEDs constructions contain AlN buffer, n-AlGaN, multi-quantum well region (GaN/AlGaN), p-AlGaN, p-GaN [9–12]. The final composition of the ternary AlGaN alloys depends on multiple parameters during growth. The most important parameters during the growth in MOVPE are pressure, gap distance (the distance between the showerhead and the susceptor in the reactor), molar flows of precursors, vapor pressure and temperature. Precise control of the Al composition during the growth of the AlGaN layer, especially of advanced structures, when fast switching between p-AlGaN/n-AlGaN and multi-quantum-wells region (which are grown in various conditions) region is necessary. The efficiency of Al incorporation into the AlGaN layer is important from a device point of view.

The aim of this study is to verify the optimal parameters for AlGaN growth with a stable 60% of Al and to determine the Al concentration deviation while changing pressure and ammonia flow.

2. Methods

The sets of the AlN/AlGaN heterostructures were grown on c-plane sapphire wafers. The structures contain 1 μm of AlN buffer and 300 nm of AlGaN layer epitaxially grown in temperature conditions 1073–1112°C. All samples were grown by metalorganic vapor phase epitaxy (MOVPE) with configuration 3 × 2" FT-CCS Flip Top Close Coupled Showerhead Aixtron reactor. Trimethylgallium (TMGa) and trimethylaluminum (TMAl) were used as metallic precursors and ammonia (NH_3) as a precursor for nitrogen. The neutral carrier gas was hydrogen (H_2). The distance between the showerhead and the susceptor (gap distance) was set to 10 mm. The experiments are divided into two sections.

TABLE I

Data collected during ammonia experiment.

Type of experiment	Sample number	NH_3 [sccm]	Pressure [mbar]	AlN/AlGaN thickness [nm]	Al content in AlGaN [%]	AlGaN relaxation [%]	Growth rate [nm/s]	Temperature on the surface during the growth [°C]
experiment with changing ammonia flow	P1	800	50	$304/987 \pm 7$	59	43.20	0.23	1075
	P2	1200		$258/970 \pm 5$	60	63.40	0.20	1112
	P3	1600		$302/987 \pm 7$	57	55.00	0.22	1073
	P4	2000		$308/987 \pm 7$	57	41.90	0.22	1078
	P5	2400		$300/987 \pm 7$	57	54.80	0.21	1078
	P6	2800		$300/987 \pm 7$	57	54.00	0.22	1077
experiment with changing pressure	P7	1200	50	$258/970 \pm 5$	60	63.40	0.20	1112
	P8		70	$300/970 \pm 5$	60	40.00	0.20	1096
	P9		90	$285/971 \pm 5$	59	46.20	0.19	1076
	P10		110	$300/987 \pm 7$	58	43.00	0.17	1075
	P11		130	$320/987 \pm 7$	57	46.80	0.16	1074
	P12		150	$294/987 \pm 7$	53	55.10	0.14	1074

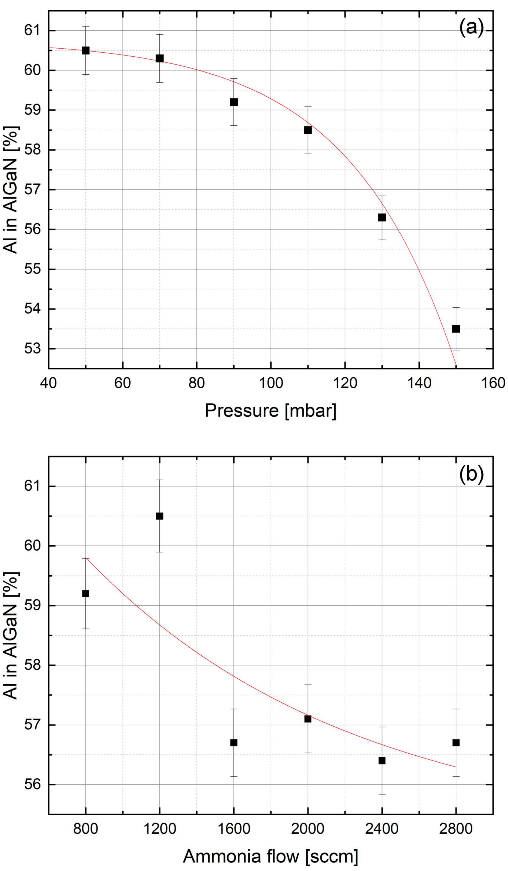

Fig. 1. The dependence on aluminium incorporation in AlGaN layer during the growth with changed parameters (a) pressure, (b) ammonia flow.

In the first part, the characteristic of the pressure dependence of AlGaN composition was studied in the pressure range from 50 mbar to 150 mbar. The step was changed every 20 mbar. In the second part, the ammonia flow was changed from 800 to 2800 sccm in steps 400 sccm, at stable pressure of 50 mbar. Table I presented all collected data from two experiments. During the experiments, only one parameter was changed during this time. For both series, the AlN buffer was grown in the same conditions. The composition of the AlGaN layers was determined by the X-ray diffraction technique. The growth rate and layer thickness was estimated using the LayTec EpiTT system based on reflectometry measurements.

3. Results and discussion

Increasing the reactor pressure caused a gradual reduction in aluminium. The difference between the two extreme points is 6% (Fig. 1a). The optimal pressure for obtaining AlGaN with a concentration of 60% is 70 mbar with the set parameters. Figure 1b shows the dependence of the amount of Al in AlGaN in relation to the change in ammonia flow during the layer growth. The aluminum content at the beginning decreases by 3–4% at higher flows, and then stabilizes.

The reflectance was measured during the growth of individual structures. The AlN growth rate reached always 0.61 nm/s due to the fact that the AlN buffer was grown under the same conditions in all samples. For the AlGaN layers grown at different pressures, a gradual decrease in the growth rate of the AlGaN layer was noted in the reflectance plot (Fig. 2). At a pressure of 50 mbar, the growth rate of the AlGaN layer was 0.20 nm/s and as the pressure increases, the growth rate decreased to a value of 0.14 nm/s at the highest pressure of 150 mbar. There is a correlation with the results obtained by Allerman and coworkers who observed that both parameters, Al composition and growth rate decreased with increasing the reactor pressure [13]. Chen's [14] and Kim's [15] groups also obtained similar results, i.e., receiving a decrease in Al incorporation into the AlGaN layer with increasing

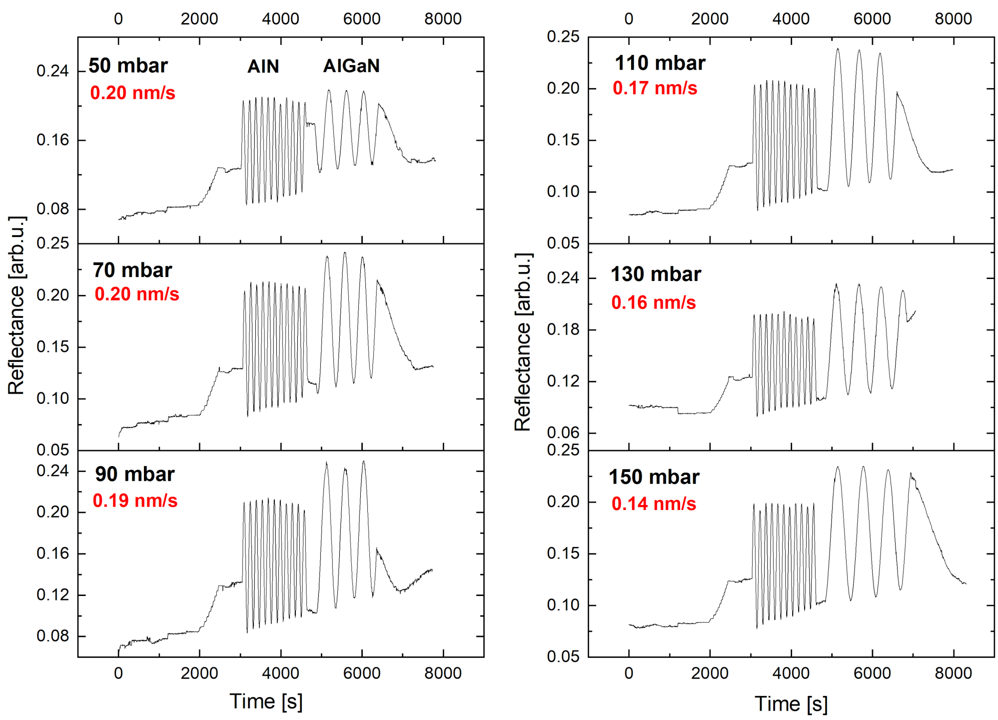

Fig. 2. The reflectance measurements were measured for wavelength 633 nm for AlGaN layers during an experiment with changing pressure. The graph includes the growth rate of AlGaN layers. The buffer AlN layer was not changed during the growth in all samples.

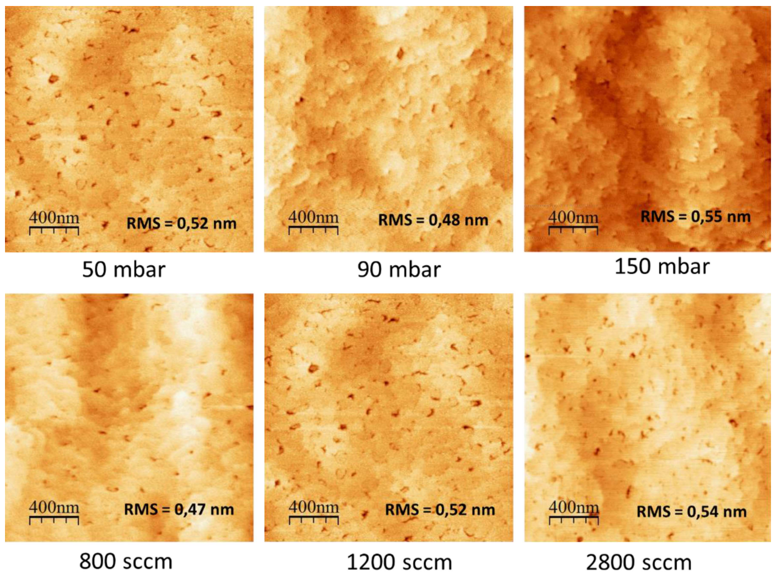

Fig. 3. The morphology of the AlGaN layers determined by using AFM technique. The scanned area is 2×2 μm, in the first row are presented samples from the experiment with changing pressure and in the second row samples from the experiment with changing ammonia flow.

pressure [16]. During the ammonia experiment, all samples were grown in 50 mbar. In the ammonia flow rate applied (800 to 2800 sccm), the observed growth rate (0.20 to 0.23 nm/s) and the change in the composition (57 to 60% of Al) changed almost by half compared to the changes observed with pressure (see Table I).

The morphology of the samples was studied by Brucker atomic force microscopy in the fast scanning mode. With increasing pressure and ammonia flow, the roughness of the samples surfaces also increases. Pressure, however, has a higher impact on the sample's surface than the ammonia flow. The topographies of all deposited structures are

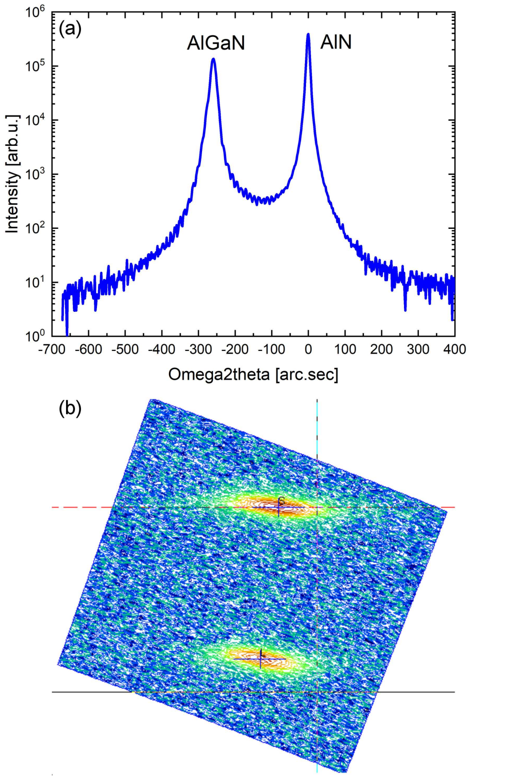

Fig. 4. XRD measurements of AlGaN layer grown in 50 mbar — symmetric scan (00.2) and reciprocal space map from asymmetric scan (01.5).

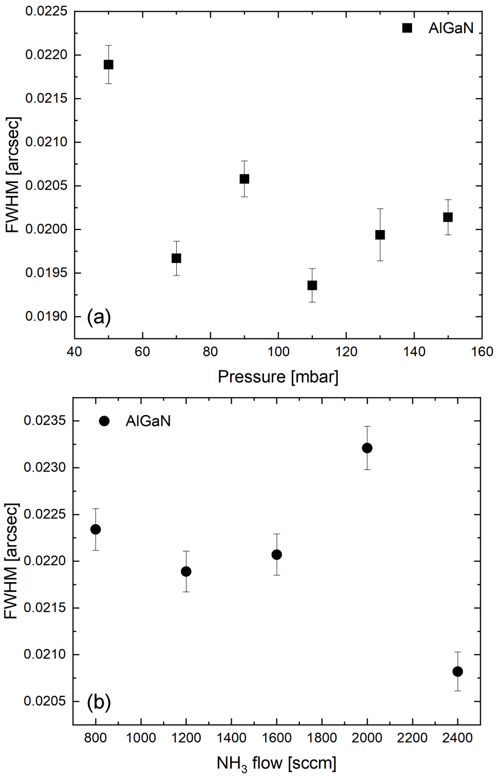

Fig. 5. Full width at half maximum (FWHM) for AlGaN layers measured from symmetrical scan (00.2).

characterized by smooth surfaces and small RMS coefficients. The surface of the structure deposited at 50 mbar shows numerous holes which disappear as the pressure increases to 90 and 150 mbar. At a pressure of 150 mbar, the growth of the AlGaN layer appears to be similar to the step-flow type growth (Fig. 3).

The crystallographic structures were determined by measurements of HRXRD. The structure quality was determined from the symmetric scan (00.2), and the relaxation and strains of the layers — from the asymmetric scan (01.5) (Fig. 4). Figure 5 presents the results of full width and half maximum (FWHM) for all AlGaN layers. AlGaN grown in 2400 sccm ammonia flow has good crystal quality due to the narrowest peak of all samples and the lowest value of FWHM. In contrast, AlGaN grown in 50 mbar has the worst crystal quality due to the highest value of FWHM.

4. Conclusions

The study presents the characteristics of $Al_{0.60}Ga_{0.40}N$ layers growth during changing conditions, pressure and ammonia flow. With increasing pressure during the AlGaN growth in the MOVPE reactor, the incorporation of aluminium is decreasing. The drop of 7% of Al was noticed in $Al_{0.60}Ga_{0.40}N$ layers in the range 50–150 mbar and a change in the growth rate (from 0.20 to 0.14 nm/s) was also observed. Ammonia flow has a lower influence on the aluminium incorporation in $Al_{0.60}Ga_{0.40}N$ layers. The aluminium content decreases by 3–4% at higher flows. Pressure has a higher impact on the sample's surface morphology and crystal quality than the ammonia flow. This is confirmed by the AFM and XRD measurements. The collected results determine what deviation should be applied when changing pressure and ammonia flow to obtain the $Al_{0.60}Ga_{0.40}N$ growth.

Acknowledgments

The study was financially supported from the project "High-performance AlGaN/GaN-HEMT transistors made with the hybrid MBE-MOVPE technology", number of agreement: 2/Ł-PORT/CŁ/2021, funded by The Łukasiewicz Centre.

References

[1] C.A. Mead, *Proc. IEEE* **54**, 307 (1966).

[2] R. Dingle, H.L. Störmer, A.C. Gossard, W. Wiegmann, *Appl. Phys. Lett.* **33**, 665 (1978).

[3] M. Kneissl, T. Kolbe, C. Chua, V. Kueller, N. Lobo, J. Stellmach, A. Knauer, H. Rodriguez, S. Einfeldt, Z. Yang, *Semicond. Sci. Technol.* **26**, 014036 (2010).

[4] M. Shatalov, W. Sun, A. Lunev, X. Hu, A. Dobrinsky, Y. Bilenko, J. Yang, M. Shur, R. Gaska, C. Moe, *Appl. Phys. Express* **5**, 082101 (2012).

[5] A.M. Armstrong, B.A. Klein, A.G. Baca, A.A. Allerman, E.A. Douglas, A. Colon, V.M. Abate, T.R. Fortune, *Appl. Phys. Lett.* **114**, 052103 (2019).

[6] K.S. Im, J.B. Ha, K.W. Kim, J.S. Lee, D.S. Kim, S.H. Hahm, J.H. Lee, *IEEE Electron Device Lett.* **31**, 192 (2010).

[7] A.M. Armstrong, B.A. Klein, A. Colon, A.A. Allerman, E.A. Douglas, A.G. Baca, T.R. Fortune, V.M. Abate, S. Bajaj, S. Rajan, *Jpn. J. Appl. Phys.* **57**, 074103 (2018).

[8] S. Kasap, P. Capper, F. Pascal, M.J. Deen, *Springer Handbook of Electronic and Photonic Materials*, Springer, 2017.

[9] R. Ni, C.C. Chuo, K. Yang, Y. Ai, L. Zhang, Z. Cheng, Z. Liu, L. Jia, Y. Zhang, *J. Alloys Compd.* **794**, 8 (2019).

[10] P.P. Michałowski, S. Złotnik, J. Sitek, K. Rosiński, M. Rudziński, *Phys. Chem. Chem. Phys.* **20**, 13890 (2018).

[11] C. Kuhn, L. Sulmoni, M. Guttmann, J. Glaab, N. Susilo, T. Wernicke, M. Weyers, M. Kneissl, *Photonics Res.* **7**, B7 (2019).

[12] S. Sumiya, Y. Zhu, J. Zhang, K. Kosaka, M. Miyoshi, T. Shibata, M. Tanaka, T. Egawa, *Jpn. J. Appl. Phys.* **47**, 43 (2008).

[13] A.A. Allerman, M.H. Crawford, A.J. Fisher, K.H.A. Bogart, S.R. Lee, D.M. Follstaedt, P.P. Provencio, D.D. Koleske, *J. Cryst. Growth* **272**, 227 (2004).

[14] C.H. Chen, H. Liu, D. Steigerwald, W. Imler, C.P. Kuo, M.G. Craford, M. Ludowise, S. Lester, J. Amano, *J. Electron. Mater.* **25**, 1004 (1996).

[15] S. Kim, J. Seo, K. Lee, H. Lee, K. Park, Y. Kim, C.S. Kim, *J. Cryst. Growth* **245**, 247 (2002).

[16] L. Tang, B. Tang, H. Zhang, Y. Yuan, *ECS J. Solid State Technol.* **9**, 024009 (2020).